

Light-induced point defect reactions of residual iron in crystalline silicon after aluminum gettering

D. Abdelbarey, V. Kveder, W. Schröter, and M. Seibt^{a)}

IV. Physikalisches Institut der Georg-August-Universität Göttingen, Friedrich-Hund-Platz 1, D-37077 Göttingen, Germany

(Received 25 June 2010; accepted 7 July 2010; published online 25 August 2010)

Deep level transient spectroscopy is used to study light-induced reactions of residual iron impurities after aluminum gettering (AIG) in crystalline silicon. White-light illumination at room temperature leads to the formation of a defect which is associated with a donor level at 0.33 eV above the valence band. This defect is stable up to about 175 °C where it dissociates reversibly in case of small iron concentrations and irreversibly for high iron concentrations. Since marker experiments using gold and platinum diffusion show a high vacancy concentration after AIG a tentative identification of the new defect as the metastable iron-vacancy pair is proposed. © 2010 American Institute of Physics. [doi:10.1063/1.3474658]

I. INTRODUCTION

Iron is one of the most frequently studied metal impurities in crystalline silicon due to its detrimental effects on the material quality and the plethora of device failures associated with various iron-related species.¹ Most prominent examples of iron-related complexes are pairs with shallow acceptors like B, Al, Ga, and In in p-type silicon materials.² Recently, research activities in the silicon photovoltaics area have renewed the interest in defect reactions of iron in B-doped crystalline silicon.³ Further developments of injection-dependent lifetime measurement techniques are now routinely used to measure concentrations of interstitial iron (Fe_i) and photoluminescence mapping is utilized to image Fe_i distributions in silicon wafers.^{4,5} Various pairs with other point defects have been reported depending on the defect population of the material under investigation, as is exemplified by FeAu pairs after Au-Fe codiffusion silicon⁶ or FeH complexes if H is introduced into the silicon by chemical etching.⁷

Due to detrimental effects of transition metal impurities, like iron, on solar cells efficiency some gettering steps are routinely included into silicon solar cells manufacturing. Standard solar cell processing include two potential gettering steps, i.e., the emitter diffusion (phosphorus-diffusion gettering, PDG) and the backsurface field formation (aluminum gettering, AIG) although the gettering capabilities are not fully exploited in present-day solar cell processing schemes. Both techniques base on an increased solubility of metal impurities in a thin surface-near gettering layer, i.e., in the highly P-doped region for PDG and in the Al-Si melt for AIG. An additional long-range beneficial effect of AIG in connection with subsequent H passivation has been attributed to the injection of vacancies (V) (Refs. 8–11) which enhances H diffusion⁹ and promotes dissociation of molecular hydrogen.¹² Such synergetic effects have been concluded to contribute to material improvement after AIG in various studies.^{13–16} From the behavior of intrinsic point defects dur-

ing silicon crystal growth¹⁷ it can be concluded that vacancies survive in complexes like V_0 , V_0O_2 , V_2 , and VH_n after AIG.

The reaction of vacancies with a typical minority carrier life-time controlling impurity like Fe_i or FeB pair in Si has been studied by electron paramagnetic resonance (EPR) and theoretical modeling.^{18–20} For these experiments 1–3 MeV electron irradiation has been used to generate vacancies, which survive in a great variety of complexes, among these—if the specimen contained Fe_i or (FeB) before irradiation—(Fe_iV) and (Fe_iV_2)-pairs and possibly Fe_s . Their atomic structure, spin states, binding, and formation energies have been determined experimentally or theoretically but their levels within the silicon band gap could not be studied experimentally because of the large variety of irradiation-induced defects.

In this paper we report a detailed deep level transient spectroscopy (DLTS) study of point defect reactions in iron containing float-zone silicon after AIG. In iron contaminated samples before and after AIG iron can be found exclusively in pairs with boron (FeB pairs) as is expected in agreement with previous data.^{21,22} However, after AIG a white-light illumination leads to the formation of an iron-related defect associated with a deep state at $E_V+0.33$ eV and subsequently referred to as the FeD defect. It is a donor as evidenced by the absence of the Poole-Frenkel effect which is expected in case of an acceptor level. In addition, a small DLTS line associated with the emission characteristics of the divacancy (V_2) appears.

The iron-related FeD defect is stable at room temperature and can be destroyed during annealing at about 175 °C leaving the V_2 -defects unaffected in accord with literature data.²³ Hence, our results provide evidence that AIG drastically changes the point defect population of crystalline silicon.

In an additional set of experiments, indiffusion of Pt or Au into silicon after AIG has been used to monitor vacancy concentrations. They consistently show strongly enhanced concentrations of substitutional Pt and Au indicating vacancy

^{a)}Electronic mail: seibt@ph4.physik.uni-goettingen.de.

concentrations as high as 10^{15} cm^{-3} after AIG. Although not a direct proof these results strongly suggest that the FeD defect is some vacancy-related Fe complex, possibly the metastable Fe_iV defect, as is discussed in detail in this paper.

II. EXPERIMENTAL

The experiments were carried out on float-zone silicon wafers ($520 \text{ }\mu\text{m}$ thickness) of p-type (boron doping $N_B = 3 \times 10^{15} \text{ cm}^{-3}$). The iron indiffusion procedure and subsequent AIG has been described in detail previously.²¹ Briefly, samples were intentionally contaminated with iron by vacuum evaporation of high purity Fe layer onto sample surface and subsequent annealing in argon atmosphere at a chosen temperature T_{ind} (between 950 and 1100 °C) for a time sufficient to guarantee uniform distribution of Fe throughout the sample. After Fe indiffusion, the samples were quenched into silicone oil (cooling rate $\approx 500 \text{ K/s}$) to freeze in the iron distribution and to prevent iron precipitation during cooling.

A surface layer of about $10 \text{ }\mu\text{m}$ thickness together with the residual FeSi_2 layer was removed from the samples surfaces by mechanical polishing with subsequent chemical etching in HF:7HNO_3 .

The AIG experiments were performed in the following way: after removing silicon oxide from the sample surfaces by a HF dip, a layer of aluminum (10 nm thick, purity: 99.999%) was thermally evaporated onto one sample surface in a vacuum better than 10^{-6} mbar. Immediately after Al evaporation, the sample was placed into a hot furnace and annealed at a chosen temperature T_{gett} equal to T_{ind} for 50 min in argon gas flow. Thereafter, samples were quenched in 10% NaOH: H_2O solution (cooling rate $\approx 2000 \text{ K/s}$) to prevent iron precipitation.

A layer of about $10\text{--}20 \text{ }\mu\text{m}$ thickness together with the Al:Si:Fe alloy formed during annealing was removed from the sample surface by mechanical polishing. DLTS was used to measure the deep level defects in our samples. For this purpose, Schottky diodes with a diameter of 1 mm for DLTS measurements were prepared by thermal evaporation of Al, while Ohmic contacts were made by rubbing an Al-Ga alloy into back surface of samples. In order to reduce the possible effects of hydrogen injection during wet etching which can result in passivation of boron atoms, FeB-pair decomposition, and formation of different hydrogen related defects with iron in the depletion region under the Schottky contact,²⁴ we used very short (10–20 s) etching in HF:7HNO_3 followed by 20 s rinsing in $\text{HF:10H}_2\text{O}$ before the evaporation of Al-Schottky contacts.

To investigate the influence of light on defect reactions and transformations we expose samples to white-light produced by a halogen tungsten lamp for durations between 15 and 45 min. We used a glass filter to eliminate the infrared components of light below 0.5–0.7 eV. Behind the filter the light intensity was about 50 mW/cm^2 which is close to the intensity of the sun light in the spectral range from 0.7 to 2.5 eV. According to our estimations based on results by Geerligs and MacDonald,³ this light treatment was enough to guarantee dissociation of more than 95% of FeB pairs to a depth corresponding approximately to the minority carrier

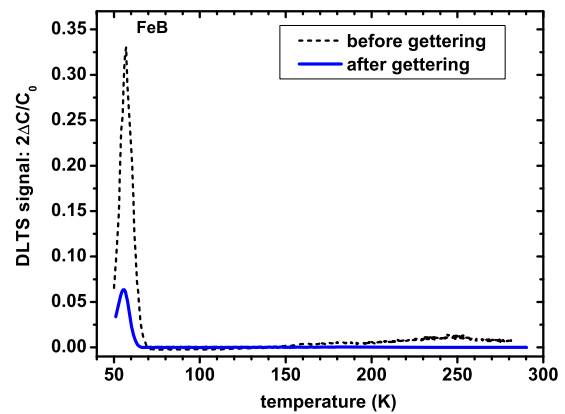


FIG. 1. (Color online) DLTS spectra of iron in silicon after indiffusion at 1050 °C (dashed line) and after subsequent AIG at 1050 °C (solid line); both high temperature treatments have been terminated by rapid quenching. Both spectra show iron as FeB pairs as the dominant signal. It is clearly seen that AIG reduces the iron concentration in accord with previously published data (Ref. 21).

diffusion length, i.e much deeper than the depth of our DLTS measurements even for concentrations of iron as high as $2 \times 10^{14} \text{ cm}^{-3}$.

To estimate the initial vacancy concentration $[V]_{\text{init}}$ in our samples we performed gold indiffusion for 2 h at 850 °C or platinum indiffusion at 730 °C for 30 min into the same Si wafer we used for iron experiments but without the initial iron indiffusion. We performed these experiments before and after AIG. The latter was performed for 50 min at 1100 °C using Al layer thicknesses of 10 and 400 nm. The layer of $30 \text{ }\mu\text{m}$ together with Al:Si alloy was removed after AIG and Au was subsequently evaporated on this freshly etched surface. After Au indiffusion a surface layer with a thickness ranging from 20 to $150 \text{ }\mu\text{m}$ was removed by mechanical polishing and DLTS spectra were measured. Similar experiments have been carried out using Pt indiffusion at 730 °C for 30 min using the same preparation procedure as for the Au indiffusion.

DLTS spectra have been recorded using a Boonton B72 capacitance meter operating at 1 MHz. All spectra shown in this paper have been measured at 5 V bias voltage, 4 V pulse voltage, 261 Hz pulse repetition frequency, and a pulse length of 100 μs .

III. RESULTS

Figure 1 shows, as an example, typical DLTS spectra measured in one of our samples before and after AIG at $T_{\text{gett}} = T_{\text{ind}} = 1050 \text{ }^\circ\text{C}$. In both spectra (FeB) pairs with a donor energy level at about $E_V + 0.1 \text{ eV}$ are dominant in the spectra, while the signal from the Fe_i donor (at $E_V + 0.39 \text{ eV}$) as well as the signals from any other possible electrically active species are nearly negligible. From such kind of measurements the segregation coefficient for AIG can be calculated depending on gettering temperature as was done in our previous paper.²¹

It is well established that if the concentration of interstitial iron is much smaller than the boron concentration ($[\text{Fe}_i] \ll N_B$) in p-type silicon, Fe_i atoms become trapped by substitutional boron forming a complex $\text{Fe}_i^{(+)}\text{B}_s^{(-)}$ essentially

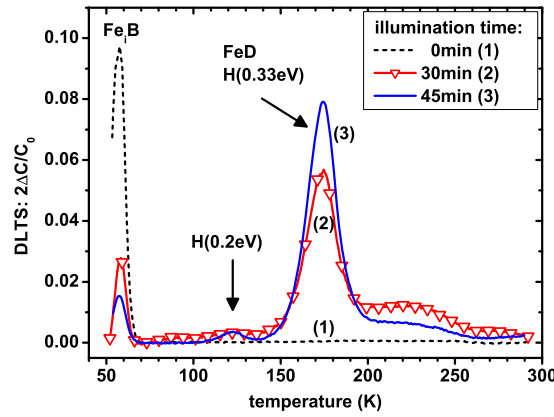


FIG. 2. (Color online) DLTS spectra showing the effect of cold-light illumination on residual iron after AIG at 1100 °C. Initially, iron is found in form of FeB pairs [(1), dashed line]. Room temperature illumination using white-light (50 mW/cm²) for 30 min [(2), solid line and triangles] leads to a decrease in the FeB-line and a simultaneous increase in the line labeled “FeD” at $E_V+0.33$ eV. After 45 min of illumination [(3), solid line] nearly all iron is found in the FeD line, in addition to a small DLTS signal corresponding to a defect at $E_V+0.2$ eV.

bound by Coulomb interaction. For the concentrations of iron and boron in our samples, complete pairing of Fe_i is expected at room temperature. The characteristic time constant of this first order reaction is estimated according to Ref. 25 for the boron doping in our samples and for room temperature as 2.5 h. Typically, more than seven hours elapsed between annealing or illumination and the DLTS measurements so that we can expect to mainly observe the DLTS signal of FeB pairs with an activation enthalpy of about $E_V+0.1$ eV.

A. Light-induced reactions of Iron

1. Formation of FeD

Figure 2 shows the DLTS spectra for the sample doped with iron and then subjected to AIG ($T_{\text{gett}}=T_{\text{ind}}=1100$ °C). Spectrum (1) was measured within a few hours after AIG, while spectra (2) and (3) within a few hours after additional white-light illumination of this sample for 30 min and 45 min, respectively. One can see that the white-light illumination results in appearance of a new DLTS peak at about 174 K, labeled as “FeD.” Furthermore, the increase in the FeD concentration correlates well with a decrease in the concentration of FeB pairs. It should be explicitly mentioned here that the same illumination of any of our samples after iron indiffusion and without AIG does not result in the appearance of the FeD line in DLTS spectra. Please note, that an additional small DLTS signal appears [H(0.2) in Fig. 2] which corresponds to a defect with an energy level at $E_V+0.2$ eV and an apparent capture cross-section of $\sigma_p \times \exp(S/k_B) = \sigma_p^* = 3 \times 10^{-15}$ cm², where S is the ionization entropy of the defect.

The activation energy for FeD defects, obtained from analysis of DLTS spectra measured at different frequencies, is 0.33 eV implying the energy level of FeD defects at $E_V+0.33$ eV. The apparent capture cross-section calculated from pre-exponential factor of the thermal emission rate is $\sigma_p^* = 3 \times 10^{-14}$ cm².

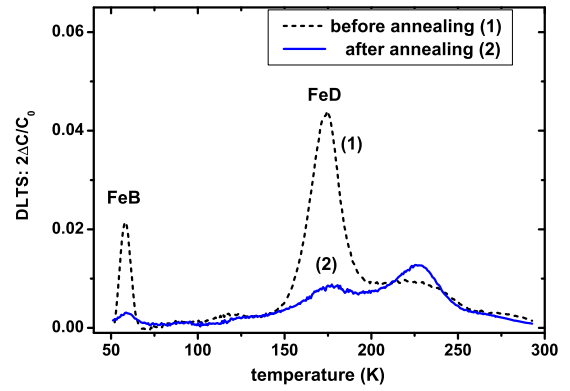


FIG. 3. (Color online) Effect of thermal annealing at 175 °C for 35 min for the case of high iron concentration ($[Fe] = 3.5 \times 10^{14}$ cm⁻³). The initial DLTS spectrum (dashed line) measured after white-light illumination shows the FeD defect as the dominant species with some iron still as FeB pairs. After annealing (solid line) both lines have almost disappeared indicating that iron has mainly precipitated.

In order to get a hint on the donor or acceptor character of this level, we have measured the hole emission rate of FeD defects at two different average electric fields in the depletion region of the Schottky contact: $\mathcal{E}_1 = 3.9 \times 10^4$ V/cm ($U_b = 5$ V, $U_p = 5$ V) and $\mathcal{E}_2 = 2.0 \times 10^4$ V/cm ($U_b = 5$ V, $U_p = 1.5$ V). For $T = 175$ K the emission rate was 613 s⁻¹ at \mathcal{E}_1 and 603 s⁻¹ at \mathcal{E}_2 , that is the same within experimental accuracy implying the FeD defect to be a donor. For an acceptor level one expects an increase in emission rate by about factor 1.35 with increase in electric field from \mathcal{E}_2 to \mathcal{E}_1 due to the Poole–Frenkel effect.²⁶

2. Dissociation of FeD

In order to estimate the thermal stability of FeD defect we made annealing experiments. Figure 3 shows the results for one of our samples, where the Fe indiffusion with subsequent AIG were made at $T_{\text{gett}}=T_{\text{ind}}=1100$ °C. The sample was first illuminated to generate FeD defects. The initial concentration of iron before illumination was of about 3.5×10^{14} cm⁻³. Spectrum (1) was measured before annealing and spectrum (2) after annealing at 175 °C for 35 min. Annealing at 175 °C for 35 min results in a dramatic reduction in concentrations of both FeB and FeD defects. The reduction in FeB concentration is not surprising and can be easily understood assuming thermal dissociation of FeB pairs and a subsequent precipitation of Fe_i in accord with previous investigations.²⁷

Two reaction paths, however, can account for the decrease in the FeD concentration, i.e.,

- 1 dissociation of FeD producing Fe_i and its subsequent precipitation, or
- 2 the transformation from a metastable defect (FeD) into a more stable configuration which cannot be detected by DLTS in p-type silicon.

It is clear that these paths cannot be distinguished on the basis of experimental data presented above. Reaction path (2) should be independent on the total iron concentration while a reaction along path (1) can be reduced or even suppressed by a reduction in the iron concentration. Hence,

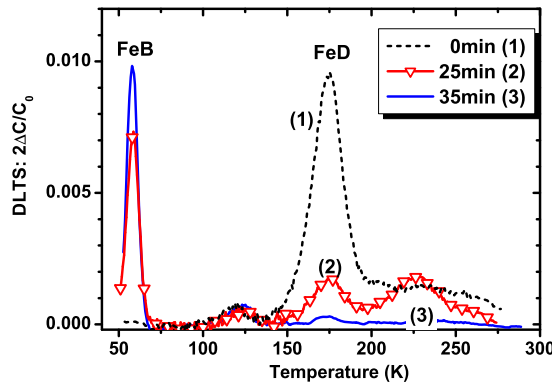


FIG. 4. (Color online) Effect of thermal annealing at 175 °C for the case of small iron concentration ($[Fe] \approx 4 \times 10^{13} \text{ cm}^{-3}$). The initial DLTS spectrum [(1), dashed line] measured after white-light illumination shows the FeD defect as the dominant species with some iron still as FeB pairs. After annealing at 175 °C for 25 min [(2), triangles and solid line] and 35 min [(3), solid line] the FeD signal has decreased which is accompanied by a respective increase in the FeB signal. Hence, the thermal dissociation reaction is reversible for small iron concentrations.

these experiments have been repeated with samples containing only about 10% iron after AIG. Figure 4 shows the results of annealing experiments with a sample which was iron diffused and gettered at 1000 °C ($T_{\text{gett}} = T_{\text{ind}} = 1000 \text{ °C}$) resulting in an iron concentration after AIG of about $4 \times 10^{13} \text{ cm}^{-3}$, i.e., about one order of magnitude below the data presented in Fig. 3. Under these conditions the decrease in the FeD concentration is accompanied by an *increase* in the FeB concentration implying a reversible reaction. Hence, we can conclude that annealing at 175 °C dissociates the FeD defect producing mobile Fe_i which then precipitates or forms FeB pairs during room temperature storage for large and small iron concentrations, respectively.

B. Marker experiments using Au and Pt diffusion

Since the light-induced formation of the FeD line was exclusively observed in samples subjected to an AIG treatment, this procedure has to change the defect spectrum of silicon wafers. In addition, these changes are far-reaching since DLTS has been measured up to 100 μm below the surface opposite to the Al layer used for gettering, i.e., at least at a distance of 200 μm away from the gettering layer. This excludes a possible *direct effect* of Al atoms themselves since the Al diffusion coefficient in Si is small and Al cannot diffuse into Si during AIG annealing more than a few microns.²⁸

A long-range effect of AIG in addition to the pure gettering effect has been observed in multicrystalline silicon for photovoltaics as a synergetic action of AIG and hydrogen passivation from a SiN_x layer produced by plasma-enhanced chemical-vapor deposition.^{8,15} It has been attributed to the production of vacancies during AIG resulting from the formation of liquid AlSi above the eutectic temperature of 577 °C, an interpretation that has not been supported by later platinum diffusion experiments performed on different silicon materials.²⁹ This method was proposed by Zimmermann and Rysse³⁰ and further developed by Jacob *et al.*³¹

and is able to quantify the initial vacancy concentration $[V]_0$ present in silicon samples at the onset of platinum or gold diffusion.

In order to estimate vacancy concentrations after AIG in our samples we performed gold and platinum indiffusion as marker experiments. Our preliminary experiments include two different Al layer thicknesses of 10 nm—used also for the experiments described above— and of 400 nm. In the latter case, the effect is huge, $[V]_0 \approx (2-3) \times 10^{15} \text{ cm}^{-3}$, while for the thin Al layer of 10 nm it is smaller but still significant between 4×10^{13} and 10^{14} cm^{-3} .

IV. DISCUSSION

A. General conclusions

The results described above first of all show that point defect reactions of iron in boron-doped float-zone silicon after AIG are fundamentally different from the well-known pairing of its interstitial species with substitutional boron. Hence, it can be concluded that AIG substantially changes the defect spectrum of the material. Preliminary marker experiments further show a considerably higher vacancy concentration after AIG indicating that vacancy-related defects are responsible for the observed light-induced reaction of interstitial iron.

According to Ref. 3 the intensity of the white-light illumination used in our experiments is sufficient to almost completely dissociate FeB pairs in a few minutes within the depth of about one electron diffusion length. Therefore, a reasonable conclusion is that FeD defects appear due to the reaction of an unknown species with Fe_i atoms rather than a reaction with existing FeB pairs. In addition to the dissociation of FeB pairs, white-light illumination may also lead to a radiation enhanced defect reaction (REDR) (Ref. 32) by (i) lowering a possible reaction barrier of the FeD reaction, (ii) enhancing the diffusion of the constituents, or (iii) by optically stimulating the release of the possibly vacancy-related component from other defect vacancy complexes present after AIG and quenching.

Indeed, the fact that the light dissociates some of the V-complexes existing in our samples after AIG was directly observed in our experiments since the illumination not only produces FeD complexes but also results in the appearance of a DLTS line H(0.2) which is clearly seen in Figs. 2 and 4. It has an activation energy for hole emission of 0.20 eV and its emission characteristics are the same as those observed in Refs. 22 and 33 for the donor level of the divacancy (V_2) as is shown by a direct comparison of hole emission rates in Fig. 5. In addition, comparing the time constant for FeB pairing (150 min in our samples) with the time necessary to form FeD defects under illumination (typically 30–45 min at room temperature) provides evidence of a REDR if one bears in mind that FeD defects do not form during room temperature storage in the dark.

B. Nature of the FeD defect

Before entering a detailed discussion of vacancy-related candidates for the FeD defect we briefly want to consider a possible reaction of interstitial iron with hydrogen which

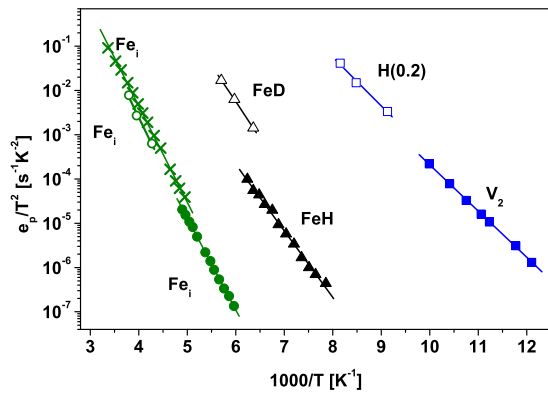


FIG. 5. (Color online) Thermal hole emission rates e_p of DLTS lines measured in this work (open symbols) compared to literature data. Our data for H(0.2) (open squares) are in agreement with emission rates reported by Brotherton *et al.* (Ref. 22) (filled squares), whereas those of FeD (open triangles) differ significantly from data reported for FeH by Sadoh *et al.* (Ref. 7) (filled triangles). The comparison of data for the Fe_i donor shows the coincidence of our data (open circles) with those of Sadoh *et al.* (Ref. 7) (filled circles) and those of Wünnel and Wagner (Ref. 11) (crosses) which corroborates the conclusion that FeD cannot be identified with FeH reported in Ref. 7.

typically is introduced during Schottky contact preparation via chemical etching. In fact, Sadoh *et al.*⁷ have reported a deep level attributed to an iron–hydrogen complex (Fe_iH). The authors observed a deep level at $E_V+0.31$ eV which is produced by chemical etching of n-type float-zone silicon containing interstitial iron. Thermal annealing at 175 °C removed the defect indicating that FeD could be identified with FeH. Thermal emission rates of the FeD defect, however, exceed those of the Fe_iH complex reported by Sadoh *et al.* by at least a factor of 20 which is an experimentally significant difference. In order to exclude discrepancies in the determination of the sample temperature between our experimental setup and that of Sadoh and co-workers, we have included data measured for Fe_i which agree within typical error margins (compare Fig. 5). It has to be concluded that FeD cannot be identified with this FeH complex.

Focusing the discussion of the possible nature of the FeD defect on iron complexes related to intrinsic point defects, oxygen and carbon, let us refer to the comprehensive theoretical treatment of Estreicher *et al.*¹⁸ as a starting point. The authors show that stable complexes of iron and *pre-existing* vacancy-related defects typically contain the substitutional iron species, i.e., Fe_s , Fe_sV , Fe_sO_i , or Fe_sB_s with the exception of the (VFeV) complex of iron and the divacancy where the iron atom sits about halfway between the two vacancies. In addition, Fe_i can be trapped in metastable configurations such as Fe_iV and Fe_iV_2 which are energetically separated by an energy barrier from the respective stable configurations Fe_s and (VFeV), respectively.

The iron-related complexes Fe_sO and Fe_iV_2 can be ruled out on the basis of their deep levels which are a donor level at $E_C-0.36$ eV (Ref. 18) and a acceptor level at $E_V+0.50$ eV,¹⁹ respectively, rather than a donor level at $E_V+0.33$ eV as observed here for the FeD defect. In addition, Fe_iV_2 complexes are stable up to 400 °C (Refs. 19 and 34) in contradiction to our data.

An intriguing candidate for the FeD defect is the metastable Fe_iV pair. This defect was experimentally found by EPR in iron contaminated silicon after high energy electron irradiation and denoted as the NL19 center.²⁰ The NL19 EPR center has a trigonal symmetry and contains one $Fe_i^{(+)}$ atom with spin 3/2. It anneals out at 160 °C in a good agreement with our experimental results for FeD.

According to our knowledge the Fe_iV complex was never investigated by DLTS and the exact position of its energy level is not known. However, it was recently investigated theoretically by Estreicher *et al.*¹⁸ showing that the Fe_iV pair should have a donor level at $E_V+0.35$ eV in a good agreement with our data for FeD. These calculations also show, however, that the Fe_iV pair should also introduce an acceptor level into the silicon band gap at $E_C-0.71$ eV. A corresponding DLTS signal has not been observed which questions the hypothesis of the Fe_iV complex as being the FeD defect. One should, however, bear in mind that the DLTS signal of a possible acceptor level close to midgap might be strongly reduced due to electron emission into the conduction band.

The dissociation kinetics—complete dissociation at 175 °C within 40 min—implies a binding energy of the FeD defect of 1.5–1.6 eV in accord with theory.¹⁸ The product of FeD dissociation is interstitial iron as can be concluded from the observed increase in the FeB concentration after annealing of a sample with a low iron concentration. As is seen in Fig. 4 such free Fe_i reacts with boron acceptors to again form FeB pairs after cooling. Considering again the Fe_iV complex the most obvious reaction path would be the direct dissociation reaction (I) $Fe_iV \Rightarrow Fe_i + V$ producing Fe_i and isolated vacancies that could readily form complexes at 175 °C. The competing *forward* reaction (II) $Fe_iV \Rightarrow Fe_s$ producing substitutional iron should, however, prevail according to the binding energies and barriers provided by theory.¹⁸ The latter might be a subject of debate since in the calculations Fe_i has been moved only along special paths and at certain velocities into the vacancy of the Fe_iV complex. In addition, one may think of an alternative dissociation path involving the diffusion of the Fe_iV defect as a whole and its reaction with e.g., an O_2 complex to form stable VO_2 and Fe_i . This scenario is in complete accord with our experiments and theoretical data¹⁸ although information about the migration of Fe_iV complexes is not available so far.

V. SUMMARY AND CONCLUSION

We have observed a light-induced reaction of residual iron in silicon after AIG leading to the formation of a new Fe species denoted as FeD. The defect is associated with a donor level at $E_V+0.33$ eV and dissociates during annealing at 175 °C. This dissociation reaction is reversible or irreversible at low and high iron concentrations, respectively. Owing to the enhanced vacancy concentration observed after AIG, we have described a tentative scenario of light-induced FeD formation and thermal dissociation involving the reaction of Fe_i and V to the metastable Fe_iV pair described theoretically by Estreicher *et al.*¹⁸ In order to be consistent with these calculations we have proposed that Fe_iV is a mobile complex

which is a hypothesis that needs to be verified or disproved by further experiments or theoretical investigations.

Vacancy injection as a result of AIG treatment has been proposed previously^{8–10} as being beneficial for subsequent hydrogen passivation treatments. The results presented here provide direct evidence for such a vacancy injection which can be concluded from gold and platinum marker experiments and the light-induced formation of V_2 . Previous marker experiments²⁹ have lead to the conclusion that no substantial vacancy injection occurs during AIG which apparently contradicts our observations. However, processing conditions as well as silicon materials used in this work and in Ref. 29 are considerably different which might lead to different results. The underlying mechanism of vacancy injection during AIG is not known so far and needs further investigations.

ACKNOWLEDGMENTS

We are especially indebted B. Schlieper-Ludewig for excellent technical support. This work was financially supported by the German Federal Ministry for the Environment, Nature Conservation, and Nuclear Safety and all the industry partners within the research cluster SolarFocus (Grant No. 0327650 B). The content of this publication is the responsibility of the authors. One of us (D.A.) gratefully acknowledges a scholarship provided by Physics Department, Faculty of Science, Menoufia University, Egypt.

- ¹A. A. Istratov, H. Hieslmair, and E. R. Weber, *Appl. Phys. A: Mater. Sci. Process.* **70**, 489 (2000).
- ²A. A. Istratov, H. Hieslmair, and E. R. Weber, *Appl. Phys. A: Mater. Sci. Process.* **69**, 13 (1999).
- ³L. J. Geerligs and D. Macdonald, *Appl. Phys. Lett.* **85**, 5227 (2004).
- ⁴R. Krain, S. Herlufsen, and J. Schmidt, *Appl. Phys. Lett.* **93**, 152108 (2008).
- ⁵D. Macdonald, A. Cuevas, and L. J. Geerligs, *Appl. Phys. Lett.* **92**, 202119 (2008).
- ⁶S. D. Brotherton, P. Bradley, A. Gill, and E. R. Weber, *J. Appl. Phys.* **55**, 952 (1984).
- ⁷T. Sadoh, K. Tsukamoto, A. Baba, D. Bai, A. Kenjo, T. Tsurushima, H. Mori, and H. Nakashima, *J. Appl. Phys.* **82**, 3828 (1997).
- ⁸A. Rohatgi, V. Yelundur, J.-W. Jeong, A. Ebong, M. D. Rosenblum, and J. I. Hanoka, *Sol. Energy Mater. Sol. Cells* **74**, 117 (2002).

- ⁹B. L. Sopori, X. Deng, J. P. Benner, A. Rohatgi, P. Sana, S. K. Estreicher, Y. K. Park, and M. A. Roberson, *Sol. Energy Mater. Sol. Cells* **41–42**, 159 (1996).
- ¹⁰L. A. Verhoef, P.-P. Michiels, W. C. Sinke, C. M. M. Denisse, M. Hendriks, and R. J. C. van Zolingen, *Appl. Phys. Lett.* **57**, 2704 (1990).
- ¹¹K. Wüstel and P. Wagner, *Appl. Phys. A: Mater. Sci. Process.* **27**, 207 (1982).
- ¹²S. K. Estreicher, J. L. Hastings, and P. A. Fedders, *Mater. Sci. Eng., B* **58**, 31 (1999).
- ¹³S. Dubois, O. Palais, M. Pasquinnelli, S. Martinuzzi, C. Jaussaud, and N. Rondel, *J. Appl. Phys.* **100**, 024510 (2006).
- ¹⁴S. Dubois, O. Palais, P. J. Ribeyron, N. Enjalbert, M. Pasquinnelli, and S. Martinuzzi, *J. Appl. Phys.* **102**, 083525 (2007).
- ¹⁵J.-W. Jeong, M. D. Rosenblum, J. P. Kalejs, and A. Rohatgi, *J. Appl. Phys.* **87**, 7551 (2000).
- ¹⁶V. Yelundur, A. Rohatgi, J.-W. Jeong, A. M. Gabor, J. I. Hanoka, and R. L. Wallace, *Proceedings of the 28th Photovoltaic Specialists Conference* (IEEE, Anchorage, 2000), p. 91.
- ¹⁷R. Falster, V. V. Voronkov, and F. Quast, *Phys. Status Solidi B* **222**, 219 (2000).
- ¹⁸S. K. Estreicher, M. Sanati, and N. Gonzalez Szwacki, *Phys. Rev. B* **77**, 125214 (2008).
- ¹⁹T. Mchedlidze and M. Suezawa, *Jpn. J. Appl. Phys., Part 1* **41**, 7288 (2002).
- ²⁰S. H. Muller, G. M. Tuynman, E. G. Sieverts, and C. A. J. Ammerlaan, *Phys. Rev. B* **25**, 25 (1982).
- ²¹D. Abdelbarey, V. Kveder, W. Schröter, and M. Seibt, *Appl. Phys. Lett.* **94**, 061912 (2009).
- ²²S. D. Brotherton, G. J. Parker, and A. Gill, *J. Appl. Phys.* **54**, 5112 (1983).
- ²³H. Hatakeyama, M. Suezawa, V. P. Markevich, and K. Sumino, *Mater. Sci. Forum* **196–201**, 939 (1995).
- ²⁴O. Feklisova, A. L. Parakhonsky, E. B. Yakimov, and J. Weber, *Mater. Sci. Eng., B* **71**, 268 (2000).
- ²⁵G. Zoth and W. Bergholz, *J. Appl. Phys.* **67**, 6764 (1990).
- ²⁶L. C. Kimerling and J. L. Benton, *Appl. Phys. Lett.* **39**, 410 (1981).
- ²⁷R. Khalil, V. Kveder, W. Schröter, and M. Seibt, *Phys. Status Solidi C* **6**, 1802 (2005).
- ²⁸D. de Cogan and Y. M. Haddara, *Properties of Crystalline Silicon*, R. Hull (ed.), (The Institute of Electrical Engineering, London, 1999), p. 599.
- ²⁹D. Karg, G. Pensl, and M. Schulz, *Proceedings of third World Conference on Photovoltaic Energy Conversion*, Osaka, May 12–16 2003, Vol. 2, pp. 1112.
- ³⁰H. Zimmermann and H. Ryssel, *Appl. Phys. Lett.* **59**, 1209 (1991).
- ³¹M. Jacob, P. Pichler, H. Ryssel, and R. Falster, *J. Appl. Phys.* **82**, 182 (1997).
- ³²L. C. Kimerling, *Solid-State Electron.* **21**, 1391 (1978).
- ³³M.-A. Trauwaert, J. Vanhellemont, H. E. Maes, A.-M. Van Bavel, G. Langouche, and P. Clauws, *Appl. Phys. Lett.* **66**, 3056 (1995).
- ³⁴B. A. Komarov, *Semiconductors* **38**, 1041 (2004).